

Synthesis of poly(diethylenetriamine terephthalamide) and its application as a flame retardant for ABS

Xingyou Chen¹ · Xufu Cai¹

Received: 7 September 2015 / Accepted: 17 February 2016 / Published online: 3 March 2016
© Akadémiai Kiadó, Budapest, Hungary 2016

Abstract A novel aliphatic–aromatic polyamide poly(diethylenetriamine terephthalamide) (PDTA) was synthesized by using terephthaloyl chloride (TPC) and diethylenetriamine (DETA). A ammonium polyphosphate (APP)/PDTA mixture was prepared for use as an intumescent flame retardant (IFR) for acrylonitrile–butadiene–styrene terpolymer (ABS). The structure of PDTA was characterized by Fourier transform infrared spectroscopy (FTIR) and ¹H NMR. The thermal properties and thermal decomposition model were investigated by differential scanning calorimetry (DSC) and thermogravimetric analysis (TG). The flame-retardant effect, thermal degradation behavior, and mechanism of IFR–ABS were investigated by limiting oxygen index (LOI), vertical burning test (UL-94), microscale combustion calorimetry test (MCC), TG, FTIR, and scanning electron microscopy (SEM). The results showed that PDTA was synthesized as expected and was stable below 200 °C. The results also showed that when the loadings of ABS, APP, and PDTA were 70, 22.5, and 7.5 %, respectively, the LOI value reached 31 % and the UL-94 vertical burning test was V-0. What is more, even when the addition of IFR was decreased to 25 %, the LOI value of the ABS/APP/PDTA (75/18.75/6.25) system was 28 %, indicating compounding APP and PDTA could improve the flame-retardant performance of ABS. The FTIR indicated there was a chemical reaction between APP and PDTA to form a heat-resistant triazine ring, and SEM

indicated the ABS/APP/PDTA systems had a denser char structure than that of pure ABS.

Keywords Poly(diethylenetriamine terephthalamide) (PDTA) · Synthesis · Acrylonitrile–butadiene–styrene terpolymer (ABS) · Intumescent flame retardant (IFR) · Flame-retardant property · Scanning electron microscopy (SEM)

Introduction

Polymer materials are used widely. However, most polymer materials are also flammable, because of which their applications are limited. As a result, it is valuable to improve the flame-retardant properties of polymer materials. Inorganic flame retardants were first used, such as Mg(OH)₂ and Al(OH)₃. However, the added amount needed was large and inorganic flame retardants had poor compatibility with polymers, limiting their application [1]. Then, organic flame retardants were developed, of which intumescent flame retardants (IFR) have been used widely. They are environment friendly and have good flame-retardant properties [2–4]. IFR are consist of a carbon source, acid source, and gas source [5–11]. Pentaerythritol (PER) and polyamides (PA) are typical carbon sources [12–15]. PER is sensitive to moisture and has poor compatibility with the polymer matrix [16, 17]. PER migrates easily to the polymer surfaces, because PER is a micromolecule. At the same time, T_m for PA is low and PA cannot disperse between polymer matrix uniformly [18].

In this paper, a novel aliphatic–aromatic polyamide, poly(diethylenetriamine terephthalamide) (PDTA), was synthesized as a charring agent (carbon resource) in our laboratory. The molecular structure was characterized by

✉ Xufu Cai
caixf2008@scu.edu.cn

Xingyou Chen
chenxingyou0417@sina.cn

¹ Department of Polymer Science and Engineering, Sichuan University, Chengdu 610065, China

FTIR and NMR. The thermal properties and corresponding thermal decomposition model were investigated by DSC and TG. PDTA is of high T_m and disperses in ABS uniformly as rigid particles. At the same time, APP was used as an acid source and gas source. APP/PDTA mixture was prepared as an IFR for acrylonitrile–butadiene–styrene terpolymer (ABS). The flame-retardant effect, thermal degradation behavior, and mechanism of IFR–ABS were investigated by limiting oxygen index (LOI), vertical burning test (UL-94), thermogravimetric analysis (TG), Fourier transform infrared spectroscopy (FTIR), and scanning electron microscopy (SEM).

Experimental

Materials

The ABS (0215A) used in this work was obtained from Jilin Petrochemical Co., Ltd (China). Ammonium polyphosphate (APP, $n > 1500$) was obtained from Zhejiang Longyou GD Chemical Industry Co., Ltd (China). Terephthaloyl chloride (TPC) was purchased from Shanghai Jinshantingxinhuagong Reagent Factory (China). Diethylenetriamine (DETA) and anhydrous lithium chloride (LiCl) were obtained from Chengdu Kelong Chemical Factory (China). Triethylamine (TEA) and N, N-dimethylacetamide (DMAC) were obtained from Tianjin Bodi Chemical Co., Ltd (China). 4A molecular sieves were obtained from Nanjing Chemical Reagent Co., Ltd (China).

Synthesis of PDTA

After the device was equipped, 40 mL DMAC treated with 4A molecular sieves was added into a dry three-necked flask. Then, anhydrous LiCl was added and agitation began. After that, a mixture including 40 mL DMAC and 2.48 g (0.024 mol) DETA was added to the flask. When the anhydrous LiCl dissolved totally, 4.87 g (0.024 mol) TPC was added into the system slowly at 0–5 °C. After the

TPC was totally added into the system, the reaction maintained for 1.5 h at 0–5 °C. Subsequently, reaction maintained for 1.5 h at room temperature. After that, 3.33 mL (0.048 mol) of TEA was added into the system to react with the HCl. And the reaction maintained for 3 h at 50 °C. After the reaction was finished, the liquid obtained was mixed with anhydrous ethanol (precipitator) as the ratio at 1:8 and the PDTA precipitated. The PDTA was dried to constant weight at 100 °C after filtration. The resulting product was light yellow. The synthesis route is illustrated in Scheme 1.

^1H NMR (D_2O): δ (ppm) 7.54 (4H, Ar–H of benzene ring), 3.77 (2H, $-\text{CH}_2-$ of being close to $\text{C}=\text{O}$), 3.45 (2H, $-\text{CH}_2-$ of being away from $\text{C}=\text{O}$). FTIR (KBr, pellet), cm^{-1} : 3289, 1549 ($-\text{NH}-$), 2943, 2701 ($-\text{CH}_2-$), 1641 ($\text{C}=\text{O}$ from $-\text{CO}-\text{NH}-$), 1293 ($\text{C}-\text{N}$), 1641, 1549, 1499, 1324 (aromatics).

Sample preparation

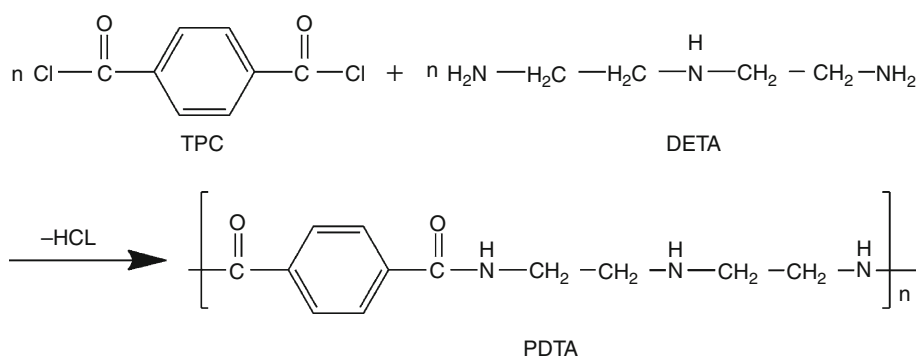
ABS, PDTA, and APP were dried in vacuum at 70 °C for 8 h before use. ABS composites with various PDTA and APP contents were prepared in a HAAKE plasticorder mixer (XSS-300, Shanghai Kechuang Rubber and Plastic Machinery Equipment Co., Ltd, China) at 195 °C and 50 rpm for 8 min. The mixed samples were transferred to the mold, preheated at 200 °C for 3 min, pressed at 10 MP, and then cooled to room temperature naturally while maintaining the pressure to obtain the composite sheets for further measurements.

Measurements

Structural characterization of PDTA

Fourier transform infrared (FTIR) spectra were recorded with a Nicolet MAGNA-IR 560 spectrometer (USA) using the KBr plate technique. ^1H NMR (400 Hz) spectra were recorded on an FT-80A NMR (Varian Corp., USA) by using D_2O as solvent.

Scheme 1 Synthesis of PDTA



Limiting oxygen index (LOI) and UL-94 tests

The LOI of all the samples was obtained at room temperature on an XYC-75 (Chengde Jinjian Analysis Instrument Factory, China) oxygen index instrument according to the GB/T240 6-93 standard. The dimensions of all the samples were $130 \times 6.5 \times 3 \text{ mm}^3$. Vertical burning rates of all samples were measured on a CZF-2 (Jiangning Analysis Instrument Factory, China) instrument, and the dimensions of all the samples were $125 \times 12.5 \times 3.2 \text{ mm}^3$, according to the UL-94 test ASTM D635-77.

Microscale combustion (MCC) test

The peak of heat release rate (pHRR) and the total heat release (THR) of the materials was obtained by MCC (FAA, Britain) test with a heat rate of $1 \text{ }^\circ\text{C/s}$ from 75 to $750 \text{ }^\circ\text{C}$. One sample was measured three times with the average value as the final result.

Thermogravimetric analysis (TG) test

TG was performed with a TG (NETZSCH TG209, NETZSCH Gerätebau GmbH, Germany) at a linear heating rate of 10 K min^{-1} . The mass of the samples was kept within 8–10 mg, and the samples were examined under air (some under nitrogen) within the temperature ranging from 50 to $700 \text{ }^\circ\text{C}$.

Scanning electron microscopy (SEM) analysis

The surface morphology of the char obtained after burning totally was observed by a scanning electron microscope (INSPECT F, FEI Corp., USA). The samples were previously coated with gold to make the surface conductible.

Fourier transform infrared (FTIR) characterization of residual char layer

Fourier transform infrared (FTIR) spectra were recorded with a Nicolet MAGNA-IR 560 spectrometer (USA) using the KBr plate technique.

Results and discussion

PDTA synthesis and characterization of TG and FTIR

PDTA was synthesized according to a previously published procedure [19], as shown in Scheme 1. The polymerization

was carried out by reacting stoichiometric amounts of the TPC with DETA in DMAC. At the same time, adding LiCl was aimed at improving the polarity of solution, resulting in higher molecular weight being reached.

The formation of the PDTA was confirmed with ^1H NMR and FTIR. As an example, the FTIR spectrum of PDTA is presented in Fig. 1. Figure 1 shows the FTIR spectra of PDTA. In Fig. 1, the strong absorption bands at 3289 and 1549 cm^{-1} corresponded to stretching vibrations and bending vibration of N–H, respectively. The absorption bands at 2943 and 2701 cm^{-1} belong to stretching vibrations of $-\text{CH}_2-$. The absorption at 1641 cm^{-1} belongs to C=O from $-\text{CO}-\text{NH}-$ (amide I region). The absorption at 1293 cm^{-1} corresponded to stretching vibrations of C–N (amide III region). The absorption bands at 1641 , 1549 , 1499 , and 1324 cm^{-1} belong to vibrations of the benzene rings. The ^1H NMR spectrum of PDTA is shown in Fig. 2. In this figure, the peak at $\delta = 7.54 \text{ ppm}$ was assigned to the protons from benzene ring, and the peak at $\delta = 3.77 \text{ ppm}$ was assigned to the proton from the CH_2 which was close to C=O in TPC. Meanwhile, the peak at $\delta = 3.45$ was assigned to the proton from the CH_2 which kept away from C=O in TPC. What is more, the integral area ratio of chemical shift for three protons was 2:1:1, which matched with the amount of protons in PDTA.

Figure 3 shows TG and DTG curves of PDTA under nitrogen. The main datum is listed in Table 1. In Fig. 3, there was one main stage for thermal decomposition of PDTA. The T_{initial} (based on 10 % mass loss) was $328 \text{ }^\circ\text{C}$, and the main thermal decomposition temperature was between 350 and $500 \text{ }^\circ\text{C}$. The T_{max} (the temperature of peak for thermal decomposition) was $400 \text{ }^\circ\text{C}$. Scission of the main chain happened between 350 and $500 \text{ }^\circ\text{C}$. The residual carbon highly reached 27.9 %.

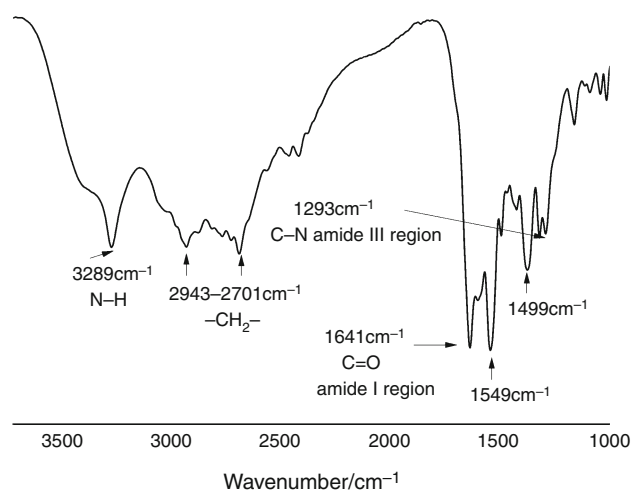


Fig. 1 FTIR spectra of PDTA

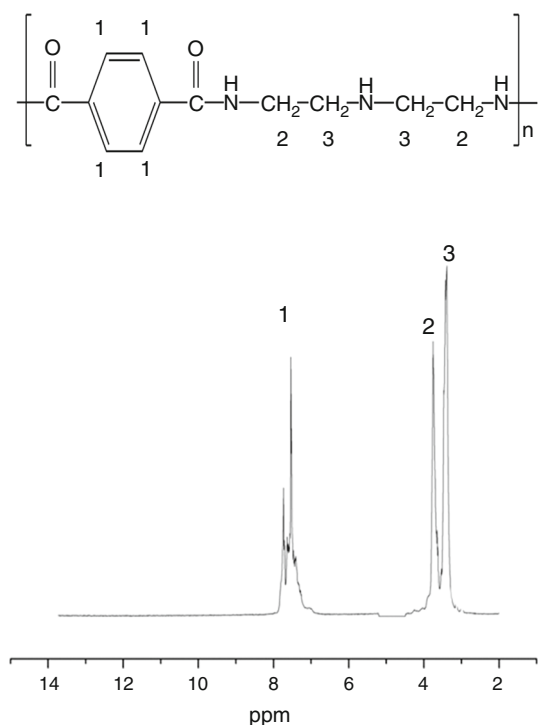


Fig. 2 ^1H NMR spectra of PDTA

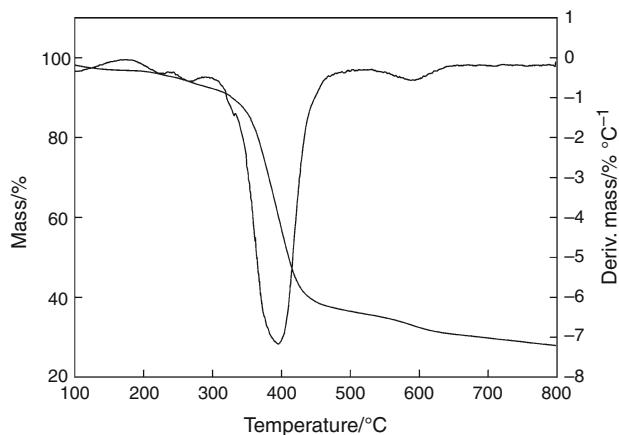


Fig. 3 TG and DTG curves of PDTA

Table 1 The effect of PDTA content on combustion performance of ABS

| ABS/% | PDTA/% | APP/% | LOI/% | UL-94 |
|-------|--------|-------|-------|---------|
| 100 | – | – | 18 | No rate |
| 70 | – | 30 | 25 | No rate |
| 70 | 15 | 15 | 27 | No rate |
| 70 | 10 | 20 | 29 | V-2 |
| 70 | 7.5 | 22.5 | 31 | V-0 |
| 70 | 6 | 24 | 29 | V-1 |
| 70 | 5 | 25 | 29 | V-1 |

Table 2 The effect of IFR content on combustion performance of ABS

| ABS/% | PDTA/% | APP/% | LOI/% | UL-94 |
|-------|--------|-------|-------|---------|
| 70 | 7.5 | 22.5 | 31 | V-0 |
| 75 | 6.25 | 18.75 | 28 | V-2 |
| 80 | 5 | 15 | 25 | No rate |

Flammability

PDTA and APP were compounded into IFR to improve the flame-retardant performance of ABS. The flame retardancy of the samples with different ratios of APP/PDTA added into the ABS was characterized by LOI and UL-94 methods. Table 1 shows the LOI values and vertical burning rates for the IFR–ABS systems. The LOI of pure ABS and ABS/APP (70/30) system was 18 % and 25 %, respectively. When the APP/PDTA loading was 30 %, the LOI values of ABS/APP/PDTA system increased first and then decreased with incremental ratio of PDTA/APP. When the loading of PDTA was 7.5 % and mass ratio of APP to PDTA reached 3:1, ABS/APP/PDTA system reached V-0 and LOI value was 31 %.

According to the results above, it indicated that the best mass ratio of APP to PDTA was 3:1. When the loadings of the IFR were decreased with the fixed ratio of APP/PDTA above, the flame retardancies of the ABS/APP/PDTA are listed in Table 2. The LOI values of ABS/APP/PDTA

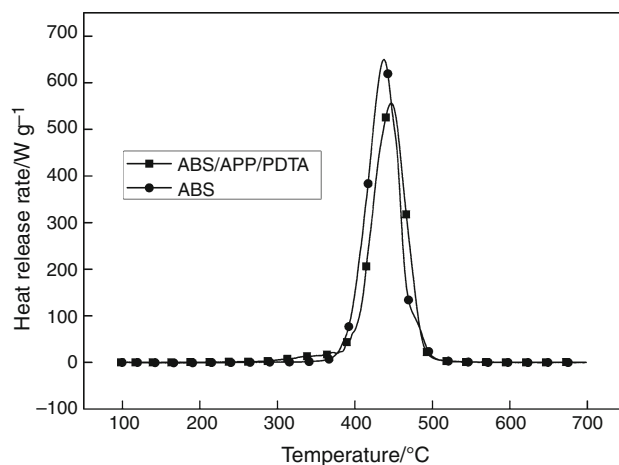


Fig. 4 The HRR curves of ABS and ABS/APP/PDTA (70/22.5/7.5)

Table 3 The pHRR and THR of ABS and ABS/APP/PDTA (70/22.5/7.5)

| Sample | pHRR/W G ⁻¹ | THR/KJ g ⁻¹ |
|----------------------------|------------------------|------------------------|
| ABS | 649.7 | 32.1 |
| ABS/APP/PDTA (70/22.5/7.5) | 556.1 | 29.2 |

system decreased with the loading of IFR. However, when the addition of IFR decreased to 25 %, the LOI value still could reach 28 %, indicating compounding APP and PDTA could improve flame-retardant performance of ABS with low loading to some extent.

Besides the LOI and UL-94 tests, MCC analysis was also used to evaluate the flame-retardant performance of ABS and ABS/APP/PDТА systems. As a laboratory-scale calorimeter, MCC can conveniently determine the flammability parameters of materials based on oxygen

consumption during combustion [20]. The HRR curves of ABS and ABS/APP/PDТА are shown in Fig. 4. At the same time, the corresponding MCC data, pHRR and THR of ABS and ABS/APP/PDТА systems, are listed in Table 3. From Fig. 4 and Table 3, it was showed that the pHRR of ABS/APP/PDТА was much smaller than that of ABS, which was only 85.5 % than that of the latter. At the same time, the THR of ABS/APP/PDТА was also smaller than that of the ABS. The pHRR and THR implied that ABS/APP/PDТА composites had a lower flame rate and more incomplete combustion degree. In accordance with the previous LOI and vertical flame test results, MCC analysis further confirmed the existence of the synergism between APP and PDТА based on the caloric variation.

Thermogravimetric Analysis

Figures 5 and 6 show the TG and DTG curves of ABS, APP, PDТА, and the ABS/APP/PDТА systems in air. Meanwhile, the main datum is listed in Table 4. In Fig. 5 and Fig. 6, the T_{initial} of pure ABS was 378 °C. The main temperature range for decomposition was between 380 and 450 °C. Meanwhile, there was only one step for thermal decomposition. The residual carbon amount of pure ABS was only 0.87 %, indicating pure ABS, itself, could not form a carbon layer. By contrast, the T_{initial} of PDТА was 118 °C and there were two main steps for thermal decomposition. The main temperature ranges for

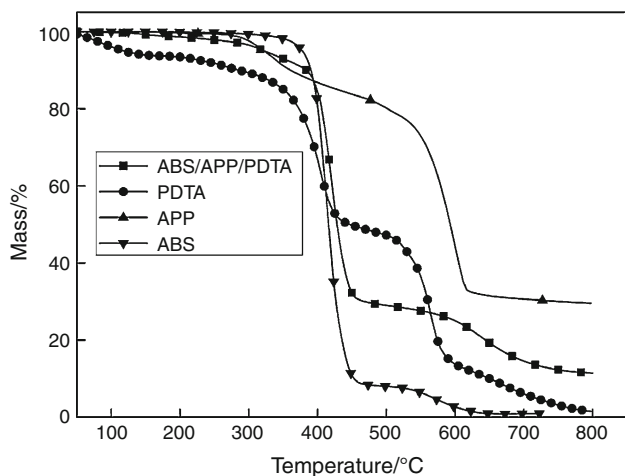


Fig. 5 TG curves of ABS, PDТА, APP, and ABS/PDТА/APP (70/22.5/7.5) in air

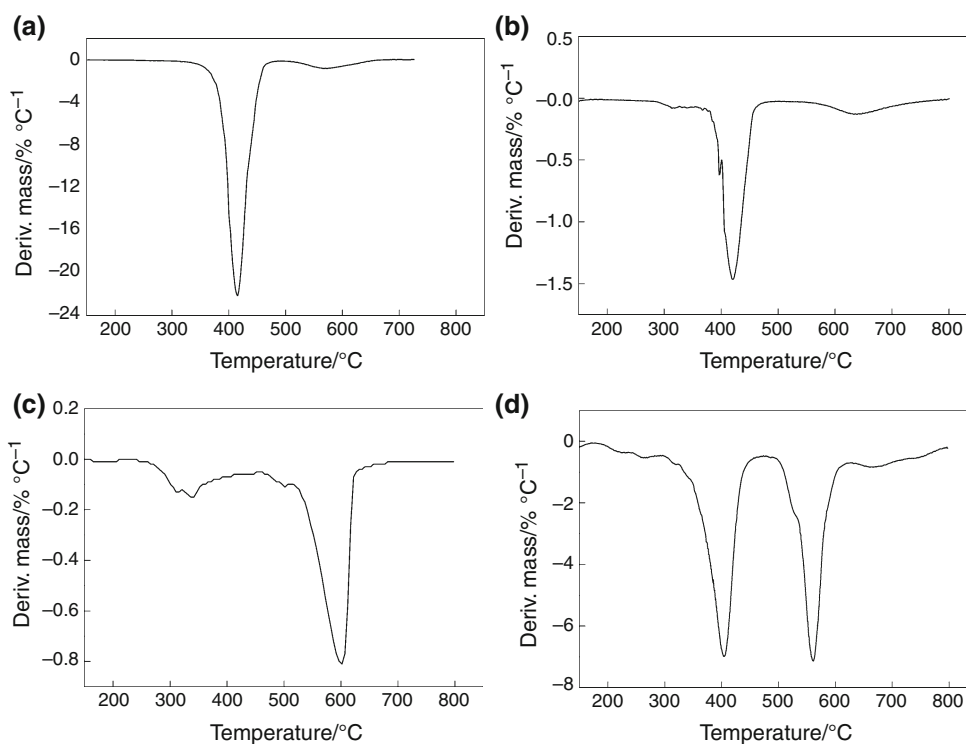


Fig. 6 DTG curves of ABS, PDТА, APP, and ABS/PDТА/APP (70/22.5/7.5) in air. **a** ABS, **b** ABS/PDТА/APP = 70/22.5/7.5, **c** APP, **d** PDТА

Table 4 TG datum of different systems under air condition

| | $T_{\text{initial}}/^{\circ}\text{C}$ | $R_{1\text{peak}}/\% \text{ } ^{\circ}\text{C}^{-1}$ | $T_{1\text{peak}}/^{\circ}\text{C}$ | $R_{2\text{peak}}/\% \text{ } ^{\circ}\text{C}^{-1}$ | $T_{2\text{peak}}/^{\circ}\text{C}$ | Char residue at 700 $^{\circ}\text{C}/\%$ | |
|----------------------------|---------------------------------------|--|-------------------------------------|--|-------------------------------------|---|------|
| | | | | | | Cal. | Exp. |
| ABS | 378 | 22.1 | 415 | – | – | – | 0.9 |
| APP | 331 | –0.2 | 342 | –0.8 | 602 | – | 24.1 |
| PDTA | 118 | –7.0 | 404 | –7.1 | 561 | – | 6.1 |
| ABS/APP/PDTA (70/22.5/7.5) | 322 | –0.6 | 397 | – | – | 8.0 | 14.6 |

T_{initial} The temperature of 5 % mass loss, $R_{1\text{peak}}$ the decomposition speed at the first decomposition peak, $T_{1\text{peak}}$ the temperature of the first decomposition peak, $R_{2\text{peak}}$ the decomposition speed at the second decomposition peak, $T_{2\text{peak}}$ the temperature of the second decomposition peak

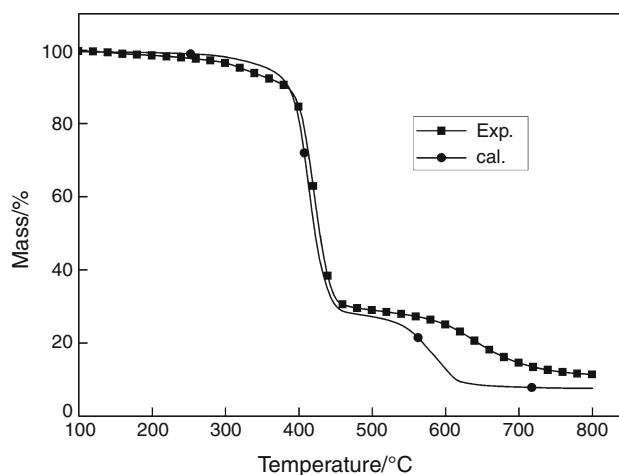
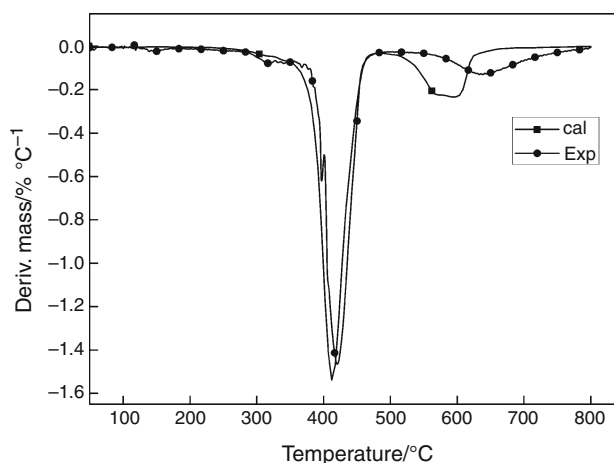
decomposition were between 380 and 430 $^{\circ}\text{C}$ and 530–600 $^{\circ}\text{C}$ separately. The residual carbon amount of PDTA was 55 % at 430 $^{\circ}\text{C}$, indicating that the main decomposition happened in the first step. The residual carbon amount of PDTA was 6.07 % at 700 $^{\circ}\text{C}$. Compared with T_{initial} of pure ABS, the T_{initial} of ABS/APP/PDTA (70/22.5/7.5) system occurred at a lower temperature and reached 322 $^{\circ}\text{C}$. What is more, the residual carbon amount of ABS/APP/PDTA (70/22.5/7.5) system reached 14.56 % at 700 $^{\circ}\text{C}$. High residual carbon amounts are important for improving flame-retardant performance. The relative amounts matched the LOI values, and vertical burning rates are listed in Tables 1 and 2.

In order to explore the effect IFR had on ABS, the experimental and calculated TG and DTG curves of the ABS/APP/PDTA (70/22.5/7.5) system are shown in Fig. 7 and Fig. 8. The main datum is listed in Table 4. At the same time, the calculated formula was as follows:

$$M_{\text{IFR/ABS}_{\text{cal}}} = w_{\text{PDTA}}\% \times M_{\text{PDTA}_{\text{exp}}} + w_{\text{APP}}\% \times M_{\text{APP}_{\text{exp}}} + w_{\text{ABS}}\% \times M_{\text{ABS}_{\text{exp}}}$$

Note: M_{cal} : calculative residual carbon amount; M_{exp} : experimental residual carbon amount; $w\%$: proportion for corresponding components.

From Figs. 7 and 8, the experimental curve of ABS/APP/PDTA (70/22.5/7.5) system was markedly different from calculated curves of ABS/APP/PDTA (70/22.5/7.5) system, indicating that the added IFR changed the thermal decomposition behavior of ABS system indeed. Firstly, the T_{initial} of ABS/APP/PDTA (70/22.5/7.5) system decreased relative to that by calculation. The temperature for the calculated calculation was 356 $^{\circ}\text{C}$, and that for the experimental value was 322 $^{\circ}\text{C}$, indicating the added IFR changed the decomposition process of the ABS/APP/PDTA (70/22.5/7.5) system. The reason we suggest was as follows: The IFR, as a catalyst, caused the thermal stability of the ABS/APP/PDTA (70/22.5/7.5) system to be worse at low temperatures and the esterification reaction between the IFR faster. However, the calculated curve was below the experimental curve above 420 $^{\circ}\text{C}$. The calculated residual carbon amount was lower than the experimental

**Fig. 7** Experimental and calculated TG curves of ABS/APP/PDTA (70/22.5/7.5) system**Fig. 8** Experimental and calculated DTG curves of ABS/APP/PDTA (70/22.5/7.5) system

residual carbon amount. The calculated residual carbon amount was 8.0 %, and the experimental residual carbon amount was 14.6 % at 700 $^{\circ}\text{C}$. As is known, a amount of residual carbon is important for the flame retardancy. In addition, it is shown in Fig. 8 that there was a

decomposition peak in the calculated DTG curve at 598 °C and the decomposition peak did not appear in experimental DTG curve. It may be because the added IFR promoted system decomposition below 400 °C. However, a steadier intermediate at high temperature was formed above 400 °C. This intermediate isolated spreading for flammable small molecules and diffusion of heat as well as oxygen, preventing lower materials decomposing. As a result, there was no decomposition peak in ABS/APP/PDPA (70/22.5/7.5) system at 598 °C. In fact, there was a decomposition peak in ABS/APP/PDPA (70/22.5/7.5) system at 625 °C, indicating that the intermediate made the decomposition temperature of the system increasing.

SEM analysis

The SEM micrographs of the char residues of the ABS/APP (70/30) and the ABS/APP/PDPA (70/22.5/7.5) are shown in Fig. 9. All the samples were combusted in air. Figure 9a shows the SEM (1000) of the ABS/APP (70/30). It was found that there were many holes and gaps on the surface. As a result, the NH_3 and CO_2 from the IFR could not be sealed off charred layer effectively to prevent heat

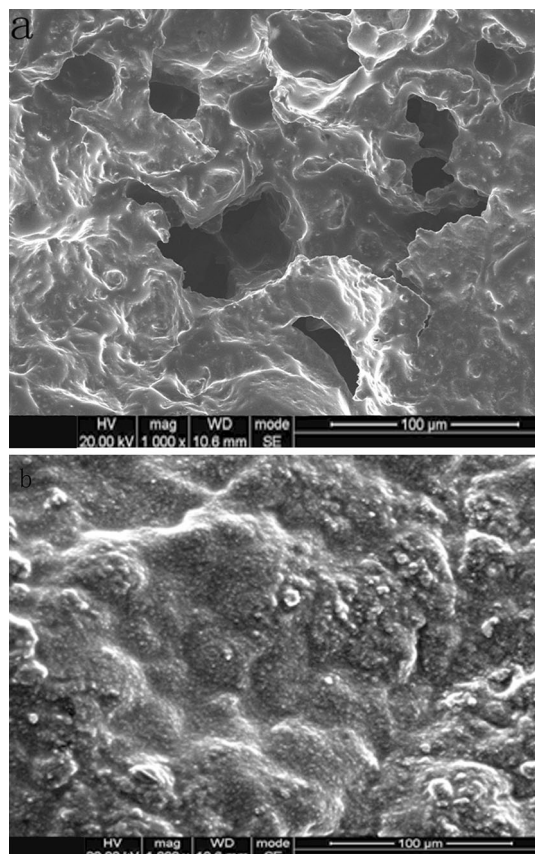


Fig. 9 SEM of the charred surface structure of ABS/APP (70/30) and ABS/APP/PDPA (70/22.5/7.5)

transmission. Figure 8b shows the SEM (1000) of the ABS/APP/PDPA (70/22.5/7.5). It was shown that the charred layer was compact and intact bulge formed by gas, resulting in insulating oxygen and heat very well.

Structural analysis of combustion residue by FTIR

In order to research the reaction mechanism of the APP/PDPA system further, those combustion residues were analyzed by FTIR. Figure 10 shows the infrared spectra of the APP/PDPA system at 25, 410, and 650 °C. At 410 °C, there were strong absorptions at 2345 and 1620 cm^{-1} , which belonged to $-\text{N}=\text{C}=\text{N}-$ and $\text{C}=\text{O}$ of $\text{O}=\text{C}=\text{N}$, while there were not those keys at 25 °C, indicating that there was reaction between APP and PDPA. The infrared spectra of APP/PDPA system at 650 °C were very simple, including only skeletal vibrations of the benzene ring, $\text{P}=\text{O}$, and $-\text{OH}$. Yin et al. [19] deduced the reactive equation of APP and PPTA, with the reactive process being expected to be almost the same between APP/PDPA and APP/PPTA. Thus, we suggest that the reactive mechanism between APP and PDPA was as follows: Firstly, phosphate esters were obtained by interaction between APP and PDPA; then, $\text{O}=\text{C}=\text{N}$ came from the intermediate generating by

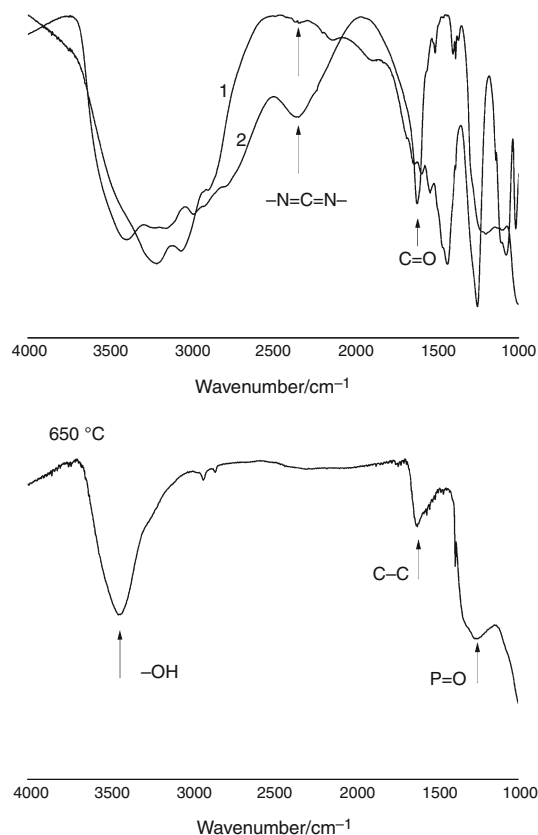


Fig. 10 FTIR spectra of the char residue of PDPA/APP for different temperatures (curve 1–25 °C, curve 2–410 °C)

interaction between phosphate ester. At the same time, interaction between $O=C=N$ and $O=C=N$ formed CO_2 and $-N=C=N-$; with the increasing temperature, the triazine ring was obtained by interaction between the $-N=C=N-$. As is known, triazine ring was heat resistant [21]. As a result, the thermal stability of the carbon layer was enhanced with triazine rings.

Conclusions

PDTA was synthesized successfully and characterized by FTIR, 1H NMR, DSC, and TG. The PDTA was used as a carbon resource, and APP was as an acid resource, being mixed to form an IFR, for improving flame-retardant performance of ABS. The addition of IFR improved the flame retardancy and changed the thermal degradation behavior of ABS. When the loadings of ABS, APP, and PDTA were 70, 22.5, and 7.5 %, respectively, the LOI value was 31 %, and the UL-94 vertical burning test ranking was V-0. Furthermore, when the addition of IFR decreased to 25 %, the LOI value of the ABS/APP/PDTA (75/18.75/6.25) system also was 28 %, indicating compounding APP and PDTA could improve the flame-retardant performance of ABS. TG curves demonstrated that the thermal stability of ABS was improved and the decomposition model was changed by adding the IFR. Moreover, the ABS/APP/PDTA system held denser char structure than that of pure ABS. At the same time, structural analysis of the combustion residue by FTIR indicated there was indeed a chemical reaction between APP and PDTA.

References

- Chen L, Cai XF. Investigation on the halogen-free flame-retardant ABS. Sichuan: Sichuan University; 2006.
- Su WG, Wu ZP. Research progress and investigation of intumescent flame retardants. *Plast Addit.* 2002;2:1.
- Wu WH, Liu S, Wang YX, Shen TF, Gao M. Thermal degradation and flame retardancy of rigid polyurethane foams containing a novel intumescent flame retardant. *J Therm Anal Calorim.* 2014;117:1419–25.
- Zhou C, Peng C, Liu L, Nie SB. Thermal oxidative degradation kinetics of novel intumescent flame-retardant polypropylene composites. *J Therm Anal Calorim.* 2015;120:1183–91.
- Wang JC, Jiang JM. Fire retardant, the newest progress and development direction of intumescent flame retardants. *Flame Retard Mater Technol.* 2001;5:5–10.
- Ou YX. Flame retardants-manufacturing, properties and applications. Peking: Weapon Industry Press; 1997. p. 169.
- Le BM, Bourbigot S. Fire retardancy of polymers: the use of intumescences. Cambridge: The Royal Society of Chemistry; 1998. p. 64.
- Baljinder KK, Horrocks AR. Complex char formation in flame retardant fiber: intumescent combinations II. Thermal analytical studies. *Polym Degrad Stab.* 1996;54:289–303.
- Zhang J, Ji KJ, Xia YZ. Polymer combustion and fire-retardant technology. Peking: Chemical Industry Press; 2005. p. 94.
- Chen XY, Sun T, Cai XF. The investigation of intumescent flame-retarded ABS using zinc borate as synergist. *J Therm Anal Calorim.* 2014;115:185–91.
- Qi SH, He MS, Li BX, Nie SB. Synergistic effects of zeolites on a novel intumescent flame-retardant low-density polyethylene (LDPE) system. *J Therm Anal Calorim.* 2013;114:581–7.
- Bourbigot Serge, Le Bras Michel. Recent advances for intumescent polymers. *Macromol Mater Eng.* 2004;289:499–510.
- Ma ZL, Gao JG, Qin JL. Effect of intumescent flame retardants on property for PP. *China Plast Ind.* 2003;31:40–2.
- Ma ZL, Zhang WY, Liu XY. Using PA6 as a charring agent in intumescent polypropylene formulations based on carboxylated polypropylene compatibilizer and nano-montmorillonite synergistic agent. *J Appl Polym Sci.* 2006;101:739–46.
- Tang Y, Hu Y, Xiao JF, et al. PA6 and EVA alloy/clay nanocomposites as char forming agents in poly(propylene) intumescent formulations. *Polym Adv Technol.* 2005;16:338–43.
- Yi JS, Lu CX. Synergistic flame retardant effect of adjuvant on the ABS/APP/PETA system. *J Chem Eng Chin Univ.* 2011;25: 319–24.
- Peng C, Yuan SJ, Zhang MX, Nie SB. Thermal and flame retardant properties of novel intumescent flame retardant polypropylene composites. *J Therm Anal Calorim.* 2013;113: 865–71.
- Wang J, Cai XF. Research progress in halogen-free intumescent flame retardants. *China Plast.* 2011;25:9.
- Yin HQ, Yuan DD, Cai XF. The high efficiency two stage intumescent contractive flame retardant on ABS. *Polym Degrad Stab.* 2013;98:288–96.
- Xu Y, Yuan L, Wang Q. Melamine polyphosphate/silicon-modified phenolic resin flame retardant glass fiber reinforced polyamide-6. *J Appl Polym Sci.* 2013;129:2171–6.
- Liu J, Liao KR, Lu ZJ. Molecular structure of triazine derivatives and relationship between structure and flame retardant property of PP. *Polym Mater Sci Eng.* 1999;15:73–5.